Journal of Medicinal Chemistry

Article

pubs.acs.org/jmc

Structural Characterization of Amorfrutins Bound to the Peroxisome Proliferator-Activated Receptor γ

Jens C. de Groot,[†] Christopher Weidner,[‡] Joern Krausze,[†] Ken Kawamoto,[§] Frank C. Schroeder,[§] Sascha Sauer,*[,‡] and Konrad Büssow*[,†]

[†]Department of Molecular Structural Biology, Helmholtz Centre for Infection Research, 38214 Braunschweig, Germany

[‡]Otto Warburg Laboratory, Max Planck Institute for Molecular Genetics, 14195 Berlin, Germany

[§]Boyce Thompson Institute and Department of Chemistry and Chemical Biology, Cornell University, Ithaca, New York, United States

Supporting Information

ABSTRACT: Amorfrutins are a family of natural products with high affinity to the peroxisome proliferator-activated receptor γ (PPARγ), a nuclear receptor regulating lipid and glucose metabolism. The PPARγ agonist rosiglitazone increases insulin sensitivity and is effective against type II diabetes but has severe adverse effects including weight gain. Amorfrutins improve insulin sensitivity and dyslipidemia but do not enhance undesired fat storage. They bear potential as therapeutics or prophylactic dietary supplements. We identified amorfrutin B as a novel partial agonist of PPARγ with a considerably higher affinity than that of previously reported amorfrutins, similar to that of rosiglitazone. Crystal structures reveal the geranyl side chain of amorfrutin B as the cause of its particularly high affinity. Typical for partial agonists, amorfrutins 1, 2, and B bind helix H3 and the β-sheet of PPARγ but not helix H12.

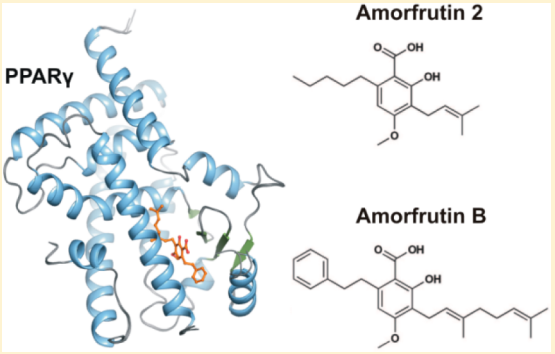

INTRODUCTION

The peroxisome proliferator-activated receptor γ (PPARγ) is a nuclear receptor that regulates transcription with two effector binding sites called activation function 1 (AF1) and activation function 2 (AF2). AF1 is localized within the N-terminal regulatory domain. The receptor's central DNA binding domain is followed by the C-terminal ligand binding domain (LBD), which comprises AF2. PPARγ is regulated by a phosphorylation site in the LBD at Ser273 (Ser245 in the shorter isoform 1).[1]

The ligand-activated transcription factor PPARγ acts in the nucleus as a heterodimer with the retinoid X receptor RXR.[2] PPARγ interacts with prostaglandins and fatty acids and their metabolites.[3−5] It acts as a sensor and regulator with a dominant role in glucose and lipid metabolism and adipose cell differentiation. Activation of the receptor improves insulin sensitivity through different metabolic actions, including regulation of adipokines.[3] PPARγ is a well-established drug target for type II diabetes. It plays also a key role in inflammation, atherosclerosis, and cancer.[3,6]

The two other PPAR family members, PPARα and PPARδ (or β), also bind fatty acids and are involved in fatty acid metabolism. In general, PPARα and PPARδ promote fatty acid catabolism in several tissues, whereas PPARγ regulates fatty acid storage in adipose tissues.[7] Dual PPARα and PPARγ agonists have been reported that correct glucose and lipid abnormalities in patients with type 2 diabetes.[8,9]

The LBD of PPARγ has several regulatory functions. It determines the receptor's subcellular localization, initiates heterodimerization with RXR, and activates or represses transcription of target genes in a ligand-dependent manner. The LBD consists of 13 α-helices and a small, four-stranded β-sheet. The lower half of the unbound LBD (Figure 2A) is structurally less rigid than the upper portion.[10,11] Helix H12 and the loop between helices H2′ and helix H3 are the most mobile segments. Ligand binding stabilizes the LBD and leads to a more compact and rigid conformation, which in turn causes recruitment of coactivators like SRC1 to the LBD's AF2 effector binding site.[1,12] PPARγ bound to the promoter of a target gene activates transcription of that target gene upon coactivator recruitment. The synthetic agonist rosiglitazone stabilizes helices H3 and H12, which are part of the AF2 site, and thereby induces coactivator recruitment.[10] Binding of rosiglitazone to the LBD also inhibits CDK5-mediated phosphorylation of Ser273, which is located in the LBD (Figure 2A).[1] Reduced Ser273 phosphorylation alters the expression of a subset of genes with regulatory functions in metabolism; for example, it increases expression of the insulin-sensitizing adipokine adiponectin.[1] The antidiabetic effects of rosiglitazone are connected with the inhibition of Ser273 phosphorylation.

Rosiglitazone and other glitazones (thiazolidinediones, TZDs) strongly activate transcription of a large number of genes in various tissues. This unspecific action of rosiglitazone is associated with its

Received: September 15, 2012
Published: January 3, 2013

dx.doi.org/10.1021/jm3013272 | J. Med. Chem. 2013, 56, 1535−1543

severe side effects including weight gain, osteoporosis, cardiovascular complications, and edema. Partial PPARγ agonists, which activate PPARγ only weakly, are more selective PPARγ modulators (SPPARγMs) and avoid side effects.[13,14] The partial agonists BVT.13, MRL-24, nTZDpa, and amorfrutin 1 block Ser273 phosphorylation as effectively as rosiglitazone but activate transcription of target genes only to a moderate level.[1,15] In contrast to full agonists, these partial agonists do not contact helix H12 but rather stabilize helix H3 and the β-sheet region of the binding pocket of the PPARγ LBD.[13]

Amorfrutins are a group of natural products that have recently been identified as PPARγ agonists with the characteristics of SPPARγMs.[15,16] Amorfrutins are nontoxic ingredients of edible roots of licorice, *Glycyrrhiza foetida*, and of the fruits of *Amorpha fruticosa*, an ingredient of condiments. They are high-affinity PPARγ agonists with dissociation constants of around 300 nM. The name "amorfrutin" is derived from the plant *Amorpha fruticosa*, in which the molecules were originally identified. The small, lipophilic amorfrutin class consists of a 2-hydroxybenzoic acid core structure decorated with phenyl and isoprenyl moieties. Amorfrutin 1 was shown to increase insulin sensitivity with concomitant weight loss in mice.[15] In contrast to rosiglitazone, amorfrutin 1 did not cause weight gain or fluid retention. Amorfrutins have potential for treatment of type II diabetes, obesity, and the metabolic syndrome in general. As components of edible biomaterials, they might also serve as prophylactic dietary supplements.

Here we present the novel PPARγ agonist amorfrutin B, which has a considerably higher affinity to PPARγ than previously described amorfrutins.[15] For understanding the cause of this high affinity, crystal structures of PPARγ in complex with amorfrutins 2 and B were solved and compared to the amorfrutin 1 complex structure reported previously.[15] The structures led to a detailed description of amorfrutin recognition by PPARγ and revealed a helix H12-independent interaction that is typical for the group of SPPARγMs.

RESULTS

Amorfrutin B Is a Novel High-Affinity Selective PPARγ Agonist. Amorfrutin B[17] was identified by a previously reported screen for potential antidiabetic substances in edible biomaterials.[15] Amorfrutin B and the previously reported amorfrutin 2 were synthesized. The dissociation constant of amorfrutin B to human PPARγ was determined as 19 nM by a time-resolved FRET assay (Table 1). In comparison to amorfrutins 1 and 2, the affinity of amorfrutin B for PPARγ is an order of magnitude stronger, comparable to that of rosiglitazone (Figure 1A, Table 1). Amorfrutins 1, 2, and B are selective for PPARγ. Two other human PPARs, PPARα and PPARδ, were bound with 60- to 140-fold lower affinity in the FRET assay (Table 1).

A fusion construct of the PPARγ LBD and the DNA binding domain of yeast GAL4 was used to measure the effect of amorfrutin B on transcription of a reporter gene. Amorfrutin B clearly activated transcription of the reporter gene (Figure 1B). Despite its high affinity for the LBD, amorfrutin B binding resulted only in a moderate level of transcriptional activation. Reporter protein production induced by amorfrutin B was 20% in comparison to rosiglitazone (Figure 1B, Table 1). Amorfrutin B therefore belongs to the group of partial agonists of PPARγ. Transcriptional activation by amorfrutin B (20%) was lower than by the partial agonists amorfrutins 1 and 2 (39%, 30%), BVT.13, MRL24, and nTZDpa (>50%) (Table 1).

Table 1. Dissociation Constants[a] (K_d), Effective Concentrations[b] (EC_{50}), and Transcriptional Activation[c] (TA) of Investigated Compounds Binding to PPAR Subtypes[d]

			PPARγ		
	PPARα, K_d [μM]	PPARδ, K_d [μM]	K_d [μM]	EC_{50} [μM]	TA [%]
amorfrutin 1[e]	27	27	0.236	0.458	39
amorfrutin 2[e]	25	17	0.287	1.200	30
amorfrutin B	2.6	1.8	0.019	0.050	20
rosiglitazone[e]	nd	nd	0.007	0.004	100
nTZDpa[e,f]	nd	nd	0.029	nd	>50
MRL-24[f]	nd	nd	nd	nd	>50
BVT.13[f]	nd	nd	nd	nd	50−80
GW7647[e]	0.001	nd	0.180	nd	nd
GW0742[e]	nd	0.0004	nd	nd	nd

[a] K_d values were obtained by using a competitive TR-FRET assay. [b] EC_{50} and transcriptional activation values were determined from a reporter gene assay. [c] TA is the maximum activation of PPARγ relative to rosiglitazone. [d] nd, not determined. [e] Value reported in ref 15. [f] Value reported in ref 13.

Structural Comparison. The crystal structures of the LBD in complex with amorfrutins B and 2 were solved by molecular replacement and were both refined to a resolution of 2.0 Å (Table 2). The electron density maps clearly reveal the domain's canonical three-layer α-helical sandwich composed of 13 α-helices and a small, four-stranded β-sheet (Figure 2A). The structures are in accord with previously published PPARγ LBD structures[8,10,13] with a calculated rms deviation of 0.87 Å to Protein Data Bank (PDB) entry 1PRG (258 common Cα-positions of chain A aligned).

The asymmetric units of crystals of PPARγ in complex with amorfrutins 1, 2, and B all contained two amorfrutin molecules bound to two LBD molecules forming a homodimer. The structures of the two monomers, denoted chain A and chain B, differ because of crystal contacts of chain B to a neighboring molecule in the crystal lattice. This conformational difference is commonly observed in PPARγ LBD structures.[8,10] In the "inactive" conformation of chain B, helix H12 is dislocated and forms crystal contacts with an adjacent molecule.[8] The "active" conformation of chain A corresponds to the structure of the receptor in complex with the full agonist rosiglitazone and the coactivator SRC1.[10] This conformation is commonly regarded as a suitable model for PPARγ LBD activation. The next sections refer to chain A and the active conformation. The inactive conformation is described in the Supporting Information file.

The electron density maps of the complex structures are well-defined for each amorfrutin molecule (Figure 2C) and clearly reveal the ligand positions in the cavity of the LBD. Corresponding to their similar structures, the three amorfrutins are bound with almost identical localization and orientation (Figure 2A,B). Whereas the full agonists rosiglitazone and MRL-20 stabilize helices H3 and H12 of the LBD,[10,13] the amorfrutins bind the receptor between helix H3 and the β-sheet, close to the ligand entry site. The recognition of the amorfrutins by PPARγ is strikingly similar to that of the partial agonists BVT.13, MRL-24, and nTZDpa.[13] The amorfrutins and the other three partial agonists all bind helix H3 and the β-sheet by a combination of hydrogen bonds to Ser342 and Arg288 and by extensive van der Waals interactions with Ile341 of the β-sheet and Cys285 of helix H3 (Figures 3, 4, and S1). The mechanism of stabilization and

dx.doi.org/10.1021/jm3013272 | J. Med. Chem. 2013, 56, 1535−1543

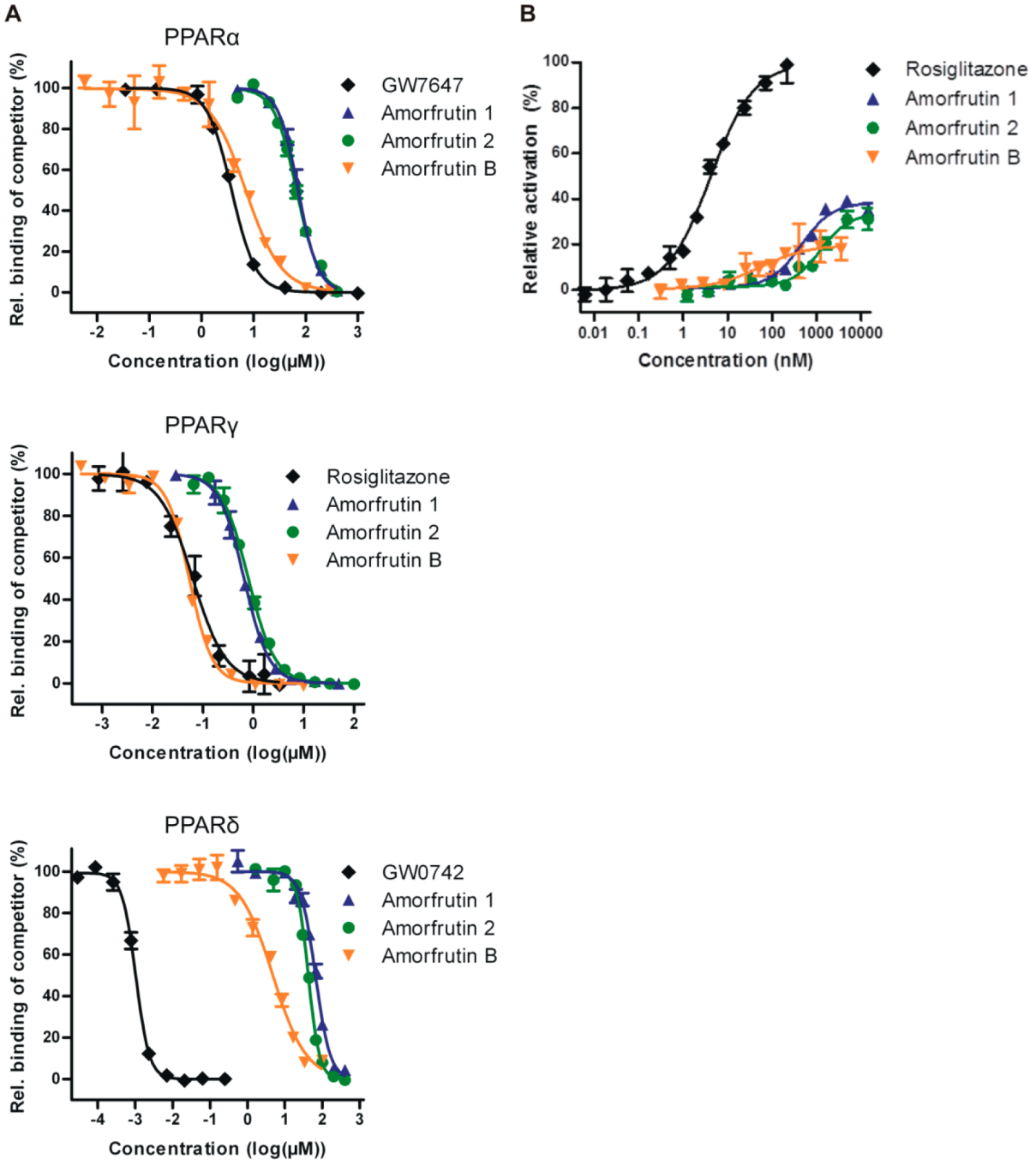

Figure 1. PPARγ binding and transcriptional activation by amorfrutins and rosiglitazone: (A) binding of compounds to the LBDs of PPARα, -γ, and -δ in a competitive, time-resolved FRET assay; (B) cellular activation of PPARγ determined in a reporter gene assay in HEK 293H cells. Error bars represent the standard deviation around the mean value (n = 3).

the low transcriptional activation (<50%) compared to the full agonist rosiglitazone[15] (Table 1) implicate amorfrutins as partial PPARγ agonists.

Despite their similar structures, the amorfrutins interact differently with the LBD. Arg288 of the amorfrutin 1-bound PPARγ adopts two alternative conformations (Figure 3), which are also observed in nTZDpa-bound PPARγ but not in unbound PPARγ (Figure 4). In the amorfrutin 1 complex, the positively charged guanidinium group of Arg288 contacts different sets of negatively charged groups depending on its conformation. The residue forms electrostatic bonds either to Glu295 of helix H3 or to Glu343 of the β-sheet and to the ligand's carboxyl group (Figure 3). Overall, Arg288 and Ser342 form a network of hydrogen bonds upon binding of amorfrutin 1 that is supported by extensive van der Waals contacts of the ligand's phenyl and isoprenyl moieties (Figure 3).

Amorfrutins 2 and B also form direct hydrogen bonds to Ser342 of the β-sheet. However, their carboxyl group does not form a salt bridge to Arg288 and they do not trigger the alternative conformation of this residue. This observation is reflected by increased crystallographic B-factors of the 2-hydroxybenzoic acid cores of amorfrutins 2 and B, which were probably caused by lower stabilization of the cores and stronger atom vibration in comparison to amorfrutin 1 (Figure 2C). Amorfrutins 2 and B use the same

dx.doi.org/10.1021/jm3013272 | J. Med. Chem. 2013, 56, 1535−1543

Table 2. Summary of Crystallographic Analysis[a]

parameter	amorfrutin B	amorfrutin 2
space group	*C*2	*C*2
cell dimensions *a*, *b*, *c* (Å)	92.14, 60.86, 117.6	92.29, 60.97, 117.9
monoclinic angle β (deg)	102.58	102.65
X-ray source	Rigaku MicroMax-007 HF	
wavelength (Å)	1.5419	1.5419
resolution range (Å)	29−2.0	27−2.0
last shell (Å)	2.10−2.00	2.10−2.00
R_{merge} (%)[b]	8.7 (45.4)	10.9 (56.3)
observations	148018 (18473)	149072 (18878)
unique reflections	42829 (5697)	43005 (5857)
mean $(I)/\sigma(I)$	17.68 (3.41)	13.71 (2.82)
completeness	99.2 (97.7)	99.0 (99.5)
multiplicity	3.5(3.2)	3.4(3.2)
structure refinement		
resolution range (Å)	29−2.0	27−2.0
R_{work} (%)[c]	20.3	20.89
R_{free} (%)[d]	23.3	25.9
total number of		
non-hydrogen atoms	4670	4671
protein atoms	4339	4380
ligand atoms	60	44
water molecules	271	247
rmsd		
bond length (Å)	0.010	0.010
bond angle (deg)	1.186	1.219
B-factors (Å^2)		
main chain	39.0	37.9
side chain	42.3	41.3
average protein atoms	40.7	39.7
average ligand atoms	43.6	47.6
average solvent	44.3	44.9
Ramachandran statistics		
most favored regions (%)	98.3	97.3
allowed regions (%)	1.7	2.7
disallowed regions (%)	0	0

[a]Values in parentheses are for the highest resolution shell. [b]$R_{merge} = \sum_{hkl}\sum_i|I_{hkl,i} - \bar{I}_{hkl}|/\sum_{hkl}\sum_i I_{hkl,i}$. [c]$R_{work} = \sum_{hkl}||F_{obs}| - |F_{calc}||/\sum_{hkl}|F_{obs}|$. [d]$R_{free}$ is calculated as R_{work} but using F_{obs} derived from 5% randomly selected reflections excluded from refinement.

residues of the LBD to form a water network that stabilizes Arg288 of helix H3 (Figure 3 and Figure S1). The partial agonist BVT.13 is bound in a similar way (Figure 4).[13] Amorfrutin 2 has a dissociation constant of 287 nM, similar to amorfrutin 1 with 236 nM, whereas binding of amorfrutin B is markedly stronger with a dissociation constant of 19 nM (Table 1). Amorfrutin B is distinguished from amorfrutin 1 by its long geranyl side chain, which forms additional hydrophobic contacts especially to Arg288 of helix H3 and to helix H4/5 (Figure 3). These additional contacts of amorfrutin B to Arg288 prevent Arg288 from adopting the alternative conformation that is required for direct contact to the compound's carboxyl group (Figure 3). The additional hydrophobic contacts are reflected by lower crystallographic *B*-factors of the geranyl side chain compared to the isoprenyl side chain of amorfrutin 1 (Figure 2C) and rationalize the almost 12-fold higher binding affinity of amorfrutin B.

Amorfrutins 1 and 2 are distinguished only by the 6-phenethyl and 6-pentyl substituents (Figure 2). The alternative conformation of Arg288 in the amorfrutin 1 complex obviously depends on the presence of its phenethyl group. However, the phenethyl/pentyl substituents are located distant from Arg288 and they do not affect the ligands' position in the binding pocket. The effect of the phenethyl/pentyl groups on Arg288 might be mediated by the flexible loop between helices H2′ and H3 or by solvent molecules.

The three amorfrutins were selectively recognized by PPARγ. Their dissociation constants were lower by a factor of 60−140 in comparison to the other PPAR subtypes in the FRET assay (Table 1).[15] The conservation of the residues of the lower portion of helix H3 and the β-sheet is quite low (Figure S1). Arg288 of PPARγ plays a key role in amorfrutin binding. The replacement of Arg288 by a threonine in PPARα and PPARδ (Figure S1) is most likely the reason why the three amorfrutins are selective for the PPARγ subtype.

DISCUSSION

The present study identified amorfrutin B as a novel high-affinity ligand of PPARγ with a dissociation constant of 19 nM, which is similar to that of rosiglitazone but significantly lower than the dissociation constants of amorfrutins 1 and 2. Therefore, amorfrutin B currently represents the natural product with the highest affinity for PPARγ.

Amorfrutins 1 and 2 and the novel amorfrutin B are recognized by PPARγ in a similar way. They bind close to the ligand entry site of the PPARγ LBD with almost identical localization and orientation. All three amorfrutins form similar, extensive van der Waals contacts with the LBD's β-sheet and helix H3. The high affinity of amorfrutins to PPARγ is caused by their carboxyl group, which interacts with the main chain nitrogen of Ser342 and, as shown for amorfrutin 1, the guanidinium group of Arg288. This is supported by the finding that esterification of the carboxyl group of the structurally related amorfrutin 5 resulted in a dramatic increase of the dissociation constant from 0.59 to 23 μM.[15] The three amorfrutins contact Ser342 by hydrogen bonds of similar strength (N−O distances 2.7−3.0 Å). The increased binding affinity of amorfrutin B in comparison to amorfrutin 1 arises from additional hydrophobic contacts of the long geranyl side chain to Arg288 of helix H3 and to helix H4/5 (Figures 3 and S1). Arg288 also seems to be crucial for the general selectivity of the amorfrutins for PPARγ over PPARα and PPARδ. Arg288 is not conserved among the PPARs. PPARα and PPARδ have a threonine at this position, which cannot interact with the amorfrutins in the same way as arginine.

Structural comparison of amorfrutins 1, 2, and B with the previously published partial PPARγ agonists BVT.13, MRL-24, and nTZDpa reveals closely related interactions with PPARγ. All of these ligands occupy the same binding site and interact similarly with helix H3 and the β-sheet. Their carboxyl groups interact directly with Ser342 of the β-sheet. Helix H3 is always stabilized by a ligand carboxyl or hydroxyl group forming a direct or a water-mediated hydrogen bond. Amorfrutins 2 and B most likely mediate PPARγ stabilization and inhibition of Ser273 phosphorylation in the same way as amorfrutin 1,[15] BVT.13, MRL-24, and nTZDpa.[1] It was shown by hydrogen/deuterium exchange experiments that MRL-24 "freezes" the region of the CDK5 phosphorylation site, apparently in a less favorable conformation for the kinase.[1]

Despite their related structures, amorfrutins 1 and 2 reveal distinct gene activation profiles.[15] Therefore, it will be important to study gene activation profiles and insulin sensitizing effects also for amorfrutin B. Amorfrutin B binds to PPARγ at markedly lower concentration than amorfrutin 1,[15] and lower doses of amorfrutin B might be sufficient for obtaining the same beneficial pharmacological effect as amorfrutin 1.

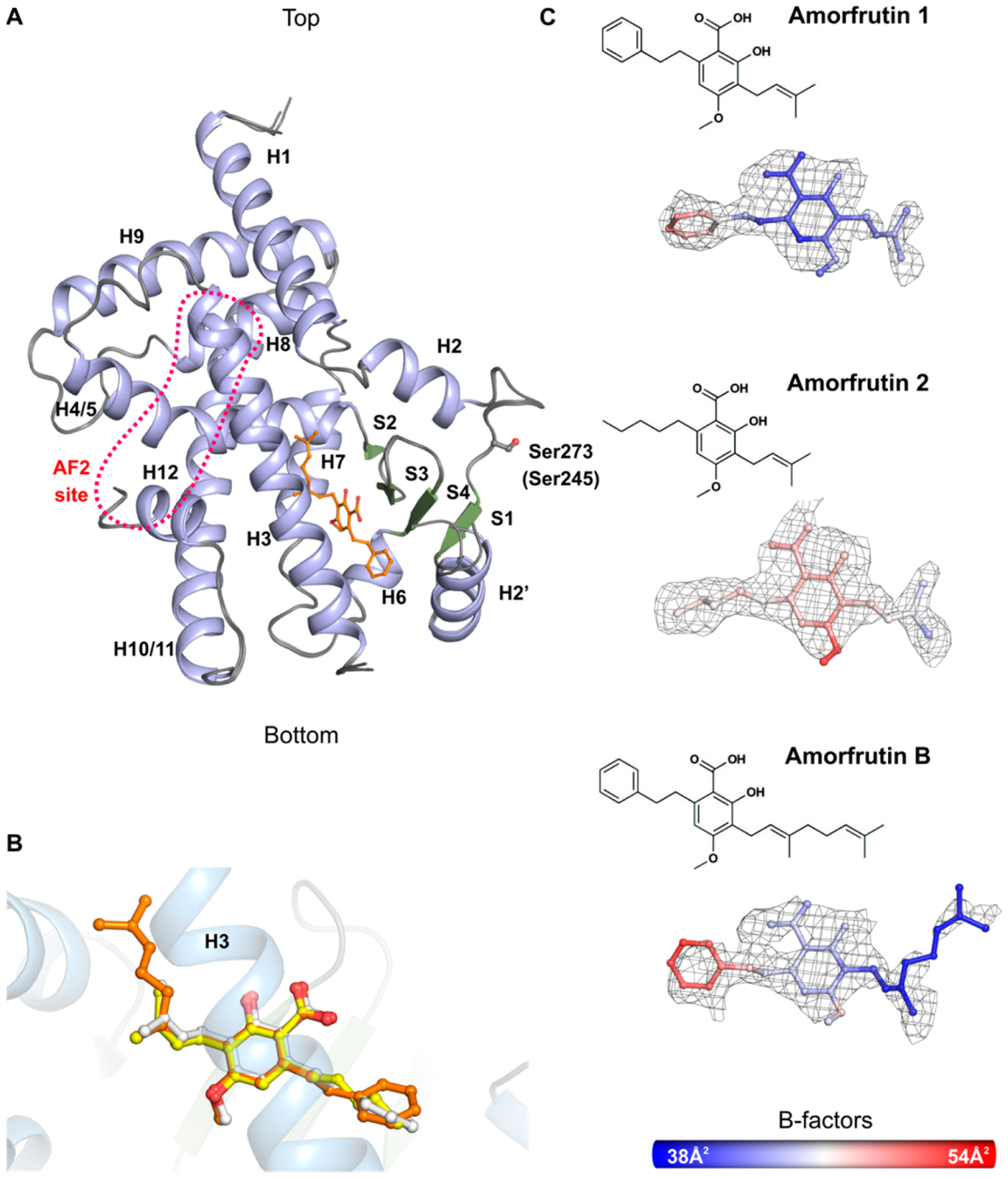

Figure 2. Structures of amorfrutins 1, 2, and B bound to the LBD of PPARγ. (A) The aligned LBD structures bound to the three amorfrutins are almost indistinguishable. Only amorfrutin B (orange sticks) is shown. The amorfrutins bind between helix H3 and the β-sheet. Helices (blue) and β-strands (green) are labeled H1−H12 and S1−S4, respectively. The phosphorylation site at Ser273 is represented by sticks (Ser273 of isoform 2 corresponds to Ser245 of isoform 1). (B) Superposition of the three amorfrutins in the binding pocket, generated by aligning the three respective protein structures. Amorfrutins 1 (PDB code 2YFE), 2, and B are shown as white, yellow, and orange sticks. Only the amorfrutin B-bound domain is displayed as ribbons. (C) $2F_O - F_C$ electron density total omit maps calculated around the amorfrutins using SFCHECK,[26] contoured at 1.0σ. The amorfrutin structures are color-coded according to the crystallographic *B*-factors (the colors range from blue to red corresponding to increasing fluctuation of atom positions). Note the low *B*-factors of the amorfrutin 1 2-hydroxybenzoic acid core in comparison to those of amorfrutins 2 and B.

CONCLUSIONS

Amorfrutins are powerful antidiabetic molecules from edible biomaterials. Amorfrutin B was identified in this study as the natural product with the highest reported affinity for PPARγ. Crystal structures of PPARγ in complex with amorfrutins 1, 2, and B reveal a highly similar binding mechanism that is related to other partial PPARγ agonists. The high affinity of amorfrutin B is caused by its carboxyl group and hydrophobic contacts of the geranyl side chain. Because of its high affinity, amorfrutin B has a high potential for treatment or prevention of type II diabetes and the metabolic syndrome.

EXPERIMENTAL SECTION

Time-Resolved Fluorescence Resonance Energy Transfer (TR-FRET) Assay. PPARγ ligands were characterized by a TR-FRET-based competitive binding assays according to the manufacturer's

dx.doi.org/10.1021/jm3013272 | *J. Med. Chem.* 2013, 56, 1535−1543

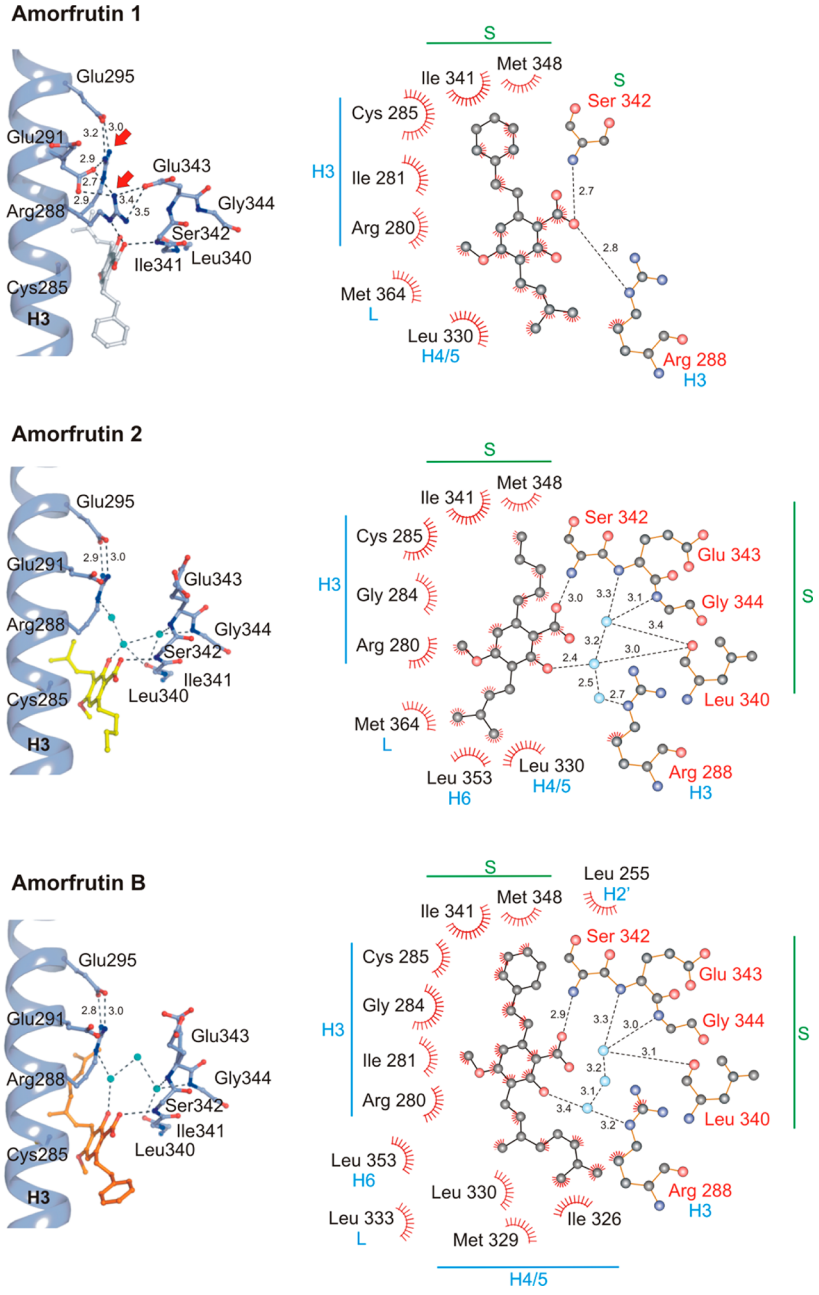

Figure 3. Structural details of amorfrutins bound to the LBD of PPARγ. Amorfrutin 1 (white) forms direct hydrogen bonds to Ser342 of the β-sheet and Arg288 of helix H3 (PDB code 2YFE). Both alternative conformations of Arg288, marked by red arrows, are stabilized by hydrogen bonds. Amorfrutins 2 and B (yellow and orange) coordinate water molecules to form hydrogen-bonding networks between Arg288 of helix H3 and the β-sheet but also directly interact with Ser342. Additional hydrophobic interactions of amorfrutin B's longer geranyl side chain to Arg288 are the likely cause of this ligand's higher binding affinity. The geranyl moiety also prevents the alternative conformation of Arg288, which was observed in the complex with amorfrutin 1. Only main chain atoms are shown for residues of the β-sheet region, excepting Glu343. In the schematic diagrams of atomic interactions on the right, calculated using LIGPLOT,[24] the ligands and PPARγ residues are drawn with black and orange bonds, respectively. Hydrogen bonds are depicted by dashed lines, and van der Waals contacts are indicated by spoked arcs and atoms with spokes. Oxygen atoms are colored red, nitrogen atoms blue, and carbon atoms black. S: β-sheet. H: helix. L: loop. Residue numbers correspond to PPARγ isoform 1. Hydrogen bonds are labeled with donor–acceptor distances in angstrom.

protocol (LanthaScreen TR-FRET PPAR Alpha/Gamma/Delta competitive binding assay kits, Invitrogen, Darmstadt, Germany), as described.[15] In the assay, increasing the concentration of potential ligands resulted in a displacement of a fluorescent PPAR ligand from fusion proteins of human PPAR LBDs with a DNA binding domain and hence a decrease of the FRET signal.

Reporter Gene Assay. Cellular activation of PPARγ was assessed in a reporter gene assay according to the manufacturer's protocol (GeneBLAzer PPARγ DA assay, Invitrogen), as described.[15] In brief, the assay uses HEK 293H cells stably expressing a GAL4-PPARγ-LBD fusion protein and an β-lactamase reporter gene under the transcriptional control of an upstream activator sequence. Cells were incubated with indicated concentrations of compounds, and β-lactamase activity was measured.

Protein Expression and Purification. The PPARγ-LBD was expressed with a previously described expression plasmid kindly provided by Krister Bamberg.[8] Transformed BL21(DE3) cells were induced with 0.1 mM IPTG at 18 °C for 20 h. Harvested cells were disrupted with a high

dx.doi.org/10.1021/jm3013272 | J. Med. Chem. 2013, 56, 1535−1543

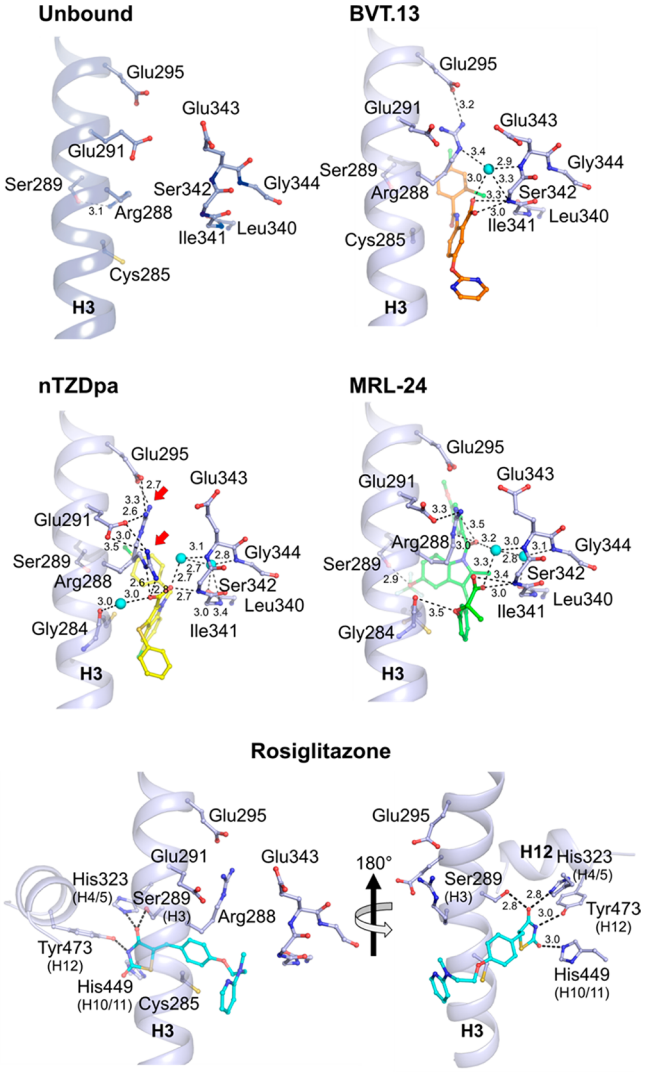

Figure 4. Comparison of related PPARγ complex structures. Shown are the unbound LBD of PPARγ (PDB code 1PRG), with Arg288 hydrogen bonded to Ser289,[10] and the LBD in complex with the partial agonists BVT.13 (2Q6S), nTZDpa (2Q5S), and MRL-24 (2Q5P).[13] The full agonist rosiglitazone (2PRG) is shown for comparison.[10] The agonists BVT.13, nTZDpa, and MRL-24 form a hydrogen bond network comprising their carboxyl groups, LBD's Arg288 and Ser342, and water molecules. These interactions are similar to the interactions of the amorfrutins. The alternative conformation of Arg288 in the nTZDpa bound state is marked by red arrows. Only main chain atoms are shown for residues of the β-sheet region, excepting Glu343. Oxygen atoms are colored red, nitrogen atoms blue, carbon atoms black, and chloride ions green. Residue numbers correspond to PPARγ isoform 1. Hydrogen bonds are labeled with donor−acceptor distances in angstrom.

pressure cell disrupter in 20 mM Tris-HCl, 150 mM NaCl, 10% glycerol, 1 mM tris(2-carboxyethyl)phosphine HCl (TCEP), 10 mM imidazole, pH 8.0, in the presence of protease inhibitors and then centrifuged. The supernatant was loaded on a 5 mL HisTrap HP column and eluted with an imidazole gradient. The eluate was diluted to 20 mM NaCl, immediately loaded onto a MonoQ HR 10/10 column, and eluted with a NaCl gradient, followed by incubation with thrombin protease (1 U/mg) at 4 °C for 20 h to cleave off the His-tag. His-tag peptides and uncleaved material were removed by rechromatography with Ni-NTA agarose, followed by Superdex 75 gel filtration in 20 mM Tris-HCl, 100 mM NaCl, 0.5 mM DTT, and 2 mM EDTA, pH 8.0.

Crystallization. The complex was prepared by adding a 10-fold molar excess of amorfrutin 1, 2, or B to the purified human PPARγ LBD at a final concentration of 1 mg/mL. DMSO and unbound ligand were removed by gel filtration. The complex was concentrated to 11 mg/mL and crystallized using hanging drop vapor diffusion by mixing it with an equal volume of reservoir solution (0.8 M trisodium citrate and 0.1 M imidazole, pH 8.0). Crystals appeared after 2−5 days at 19 °C and were improved by microseeding. The crystals were transferred into a mildly hypertonic cryoprotectant solution (0.84 M trisodium citrate, 25% v/v glycerol, and 0.1 M imidazole, pH 8.0) and immediately thereafter flash cooled in liquid nitrogen.

Structure Determination and Refinement. The data sets were collected in-house on a Saturn 944+ detector (Rigaku) using X-rays from a Rigaku MicroMax-007 HF rotating-anode X-ray generator with a VariMax Optic (Rigaku). Images were indexed and processed with XDS,[18] and the structures were solved by molecular replacement using CCP4 MOLREP[19] with ligand-free PPARγ (PDB code 1PRG)[10] as the search model. REFMAC5[20] and Phenix.refine[21] were used for refinement and Coot[22] for model building. Figures were prepared with PyMOL.[23] The schematic diagrams of atomic interactions were calculated with LIGPLOT.[24] Root mean square deviation (rmsd) values between common Cα-positions were calculated with ProFit using the McLachlan algorithm.[25]

Synthesis of Amorfrutins. Amorfrutin 1 and starting materials for the synthesis of amorfrutin B and amorfrutin 2 were synthesized as described[15] or purchased from Sigma-Aldrich or Acros Organics and used without further purification. Anhydrous solvents were prepared using 4 Å molecular sieves. Silica gel flash column chromatography was performed on Combiflash RF (Teledyne ISCO) chromatography systems using normal-phase silica gel and ethyl acetate/hexanes mixtures as solvents. ^{1}H and ^{13}C NMR spectra were obtained on 400, 500, and 600 MHz Varian NMR spectrometers using $CDCl_3$ and acetone-d_6 (Cambridge Isotope Laboratories) as solvents. The purity of the synthetic materials was assessed by proton NMR spectroscopy and HPLC. All samples were of greater than 98% purity.

(*E*)-Methyl 3-(3,7-Dimethylocta-2,6-dien-1-yl)-2-hydroxy-4-methoxy-6-phenethylbenzoate (Amorfrutin B Methyl Ester).

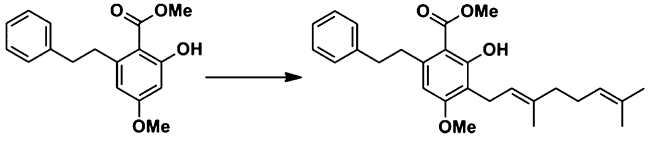

Compound 1 **Amorfrutin B methyl ester**

To a solution of methyl ester **1** (7.50 g, 26.2 mmol) in dry, distilled toluene (200 mL) under argon in a 1 L Schlenk flask was added potassium hydride (1.13 g, 28.2 mmol). The solution was stirred for 20 min at 20 °C and then heated to 70 °C. After 20 min at 70 °C the yellow reaction mixture was cooled to 20 °C, and geranyl chloride dried over molecular sieves (5.25 g, 5.64 mL, 30.4 mmol) was added. The mixture was then heated to 80 °C. The reaction was monitored by thin-layer chromatography using 3:1 hexane/ethyl acetate. After 2 h at 80 °C, the mixture was cooled to 20 °C, diluted with diethyl ether (250 mL), washed with three 100 mL portions of saturated aqueous $NaHCO_3$, and concentrated in vacuo. The crude residue was chromatographed over silica gel using a hexane/ethyl acetate solvent gradient (0% → 15%), yielding amorfrutin B methyl ester (5.00 g, 11.8 mmol, 45%) as a white solid, in addition to 3.26 g (7.7 mmol, 29%) of the O-geranylated derivative as a yellow oil. ^{1}H NMR (400 MHz, acetone-d_6): δ 11.80 (s, 1H, O<u>H</u>), 7.24−7.32 (m, 4H, phenyl), 7.16−7.22 (m, 1H, phenyl), 6.52 (s, 1H, 5-H), 5.20 (m, 1H, C<u>H</u>=C(CH_3CH_2)−CH_2−CH_2−CH=C(CH_3)$_2$), 5.06(m, 1H, C<u>H</u>=C(CH_3)$_2$), 4.01 (s, 3H, $COOCH_3$), 3.85 (s, 3H, O<u>CH_3</u>), 3.32 (d, J = 7.23 Hz, 2H, C<u>H_2</u>−CH=C(CH_3)$_2$), 3.17−3.24 (m, 2H, C<u>H_2</u>−CH_2−phenyl), 2.85−2.91 (m, 2H, CH_2−C<u>H_2</u>−phenyl), 2.06−2.07 (m, 2H, CH_2−CH_2−CH=C(CH_3)$_2$), 1.91−1.98 (m, 2H, CH_2−CH_2−CH=C(CH_3)$_2$), 1.77 (br s, 3H, CH_3), 1.61 (br s, 3H, CH_3), 1.55 (br s, 3H, CH_3) ppm. ^{13}C NMR (126 MHz, acetone-d_6): δ 173.04, 162.46, 162.26, 145.29, 143.01, 135.05, 131.56, 129.28, 129.15, 126.67, 125.12, 123.33, 115.54, 107.10, 105.91, 56.01, 52.61, 40.51, 39.96, 39.14, 27.39, 25.80, 22.48, 17.68, 16.17 ppm.

dx.doi.org/10.1021/jm3013272 | J. Med. Chem. 2013, 56, 1535−1543

(*E*)-3-(3,7-Dimethylocta-2,6-dien-1-yl)-2-hydroxy-4-methoxy-6-phenethylbenzoic Acid (Amorfrutin B).

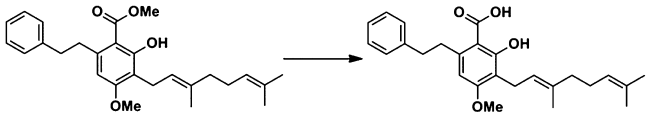

Amorfrutin B methyl ester **Amorfrutin B**

A solution of amorfrutin B methyl ester (8.57 g, 20.3 mmol) in methanol (100 mL) was added to a solution of potassium hydroxide (44 g) in a mixture of methanol (350 mL) and water (50 mL). The mixture was heated under reflux (78 °C), and progress was monitored by thin-layer chromatography. After 7 h, the mixture was cooled to 20 °C and concentrated in vacuo to a volume of 150 mL. The concentrated mixture was diluted with 200 mL of water, cooled 0 °C, and acidified (to pH 3) with 2 N aqueous hydrochloric acid. The acidic suspension was extracted with three 100 mL portions of diethyl ether. The combined ether extracts were washed with brine, dried over $MgSO_4$, and evaporated to dryness. The residue was chromatographed over silica gel using a hexane/ethyl acetate solvent gradient (0% → 20%) and then recrystallized from hexane/ethyl acetate, yielding amorfrutin B (5.75 g, 14.1 mmol, 70%) as white, sticky crystals. ^{1}H NMR (400 MHz, acetone-d_6): δ 7.22−7.31 (m, 4H, phenyl), 7.14−7.20 (m, 1H, phenyl), 6.49 (s, 1H, 5-H), 5.21 (m, 1H, C$\underline{H}$=C(CH_3CH_2)−CH_2−CH_2−CH=C(CH_3)$_2$), 5.06 (m, 1H, C$\underline{H}$=C(CH_3)$_2$), 3.85 (s, 3H, O$C\underline{H}_3$), 3.32 (d, J = 7.6 Hz, 2H, C$\underline{H}_2$−CH=C(CH_3)$_2$), 3.26−3.30 (m, 2H, C$\underline{H}_2$−CH_2-phenyl), 2.89−2.95 (m, 2H, CH_2−C$\underline{H}_2$−phenyl), 2.06−2.07 (m, 2H, CH_2−CH_2−CH=C(CH_3)$_2$), 1.91−1.98 (m, 2H, CH_2−CH_2−CH=C(CH_3)$_2$), 1.77 (br.s, 3H, CH_3), 1.69 (d, 3H, CH_3), 1.55 (br s, 3H, CH_3) ppm. ^{13}C NMR (126 MHz, acetone-d_6): δ 174.31, 163.48, 162.32, 145.94, 143.09, 134.95, 131.52, 129.24, 129.09, 126.62, 125.15, 123.32, 115.44, 106.91, 105.27, 56.00, 40.52, 39.93, 39.13, 27.38, 25.79, 22.47, 17.70, 16.21 ppm.

3-(3-Methyl-2-buten-1-yl)-2-hydroxy-4-methoxy-6-pentylbenzoate (Amorfrutin 2).

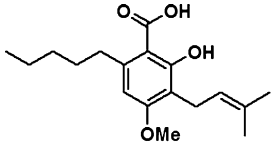

Amorfrutin 2

Amorfrutin 2 was prepared analogous to amorfrutin B, using 2-hydroxy-4-methoxy-6-pentylbenzoate instead of 2-hydroxy-4-methoxy-6-phenethylbenzoate (compound **1**). ^{1}H NMR (600 MHz, acetone-d_6): δ 6.49 (s, 1H, 5-H), 5.18 (m, 1H, C$\underline{H}$=C(CH_3)$_2$), 3.89 (s, 3H, O$C\underline{H}_3$), 3.29 (br. d, J = 7.6 Hz, 2H, C$\underline{H}_2$−CH=C(CH_3)$_2$), 2.97−3.00 (m, 2H, CH_2−C$\underline{H}_2$−phenyl), 1.74 (br s, 3H, CH_3), 1,58−1.63 (m, 5H, C$\underline{H}_2$−CH_2-phenyl and CH_3), 1.32−1.39 (m, 4H, CH_3−C$\underline{H}_2$−C$\underline{H}_2$), 0.87−0.91 (m, 3H, C$\underline{H}_3$−CH_2) ppm. ^{13}C NMR (126 MHz, acetone-d_6): δ 174.4, 163.3, 162.2, 147.2, 131.2, 123.5, 115.0, 106.5, 105.3, 56.0, 37.6, 32.8, 32.7, 25.8, 23.2, 22.4, 17.8, 14.4 ppm.

■ ASSOCIATED CONTENT

Supporting Information

Sequence alignment of the human PPAR LBDs; description of the inactive conformation of the PPARγ LBD. This material is available free of charge via the Internet at http://pubs.acs.org.

Accession Codes

PDB codes are the following: 4A4V for amorfrutin 2:PPARγ; 4A4W for amorfrutin B:PPARγ.

■ AUTHOR INFORMATION

Corresponding Author

*For S.S.: phone, +49 30 8413-1661; e-mail, sauer@molgen.mpg.de. For K.B.: phone, +49 531 6181-4550; e-mail, konrad.buessow@helmholtz-hzi.de.

Notes

The authors declare no competing financial interest.

■ ACKNOWLEDGMENTS

The authors thank Thorsten Lührs for asymmetric flow field-flow fractionation and Manfred Nimtz and Undine Felgenträger for mass spectrometry experiments. This work is part of the Ph.D. theses of J.C.d.G. and C.W. Our work is supported by the German Ministry for Education and Research (BMBF, Grant 0315082), the National Genome Research Net (NGFN, Grant 01 GS 0828), the European Union ([Grant FP7/2007-2011], under Grant Agreement No. 262055 (ESGI)), the Max Planck Society and the Helmholtz Centre for Infection Research.

■ ABBREVIATIONS USED

AF, activation function; LBD, ligand binding domain; PPAR, peroxisome proliferator-activated receptor; RXR, retinoid X receptor; SPPARγM, selective peroxisome proliferator-activated receptor γ modulator

■ REFERENCES

(1) Choi, J. H.; Banks, A. S.; Estall, J. L.; Kajimura, S.; Bostrom, P.; Laznik, D.; Ruas, J. L.; Chalmers, M. J.; Kamenecka, T. M.; Bluher, M.; Griffin, P. R.; Spiegelman, B. M. Anti-diabetic drugs inhibit obesity-linked phosphorylation of PPARγ by Cdk5. *Nature* **2010**, *466*, 451−456.

(2) Berger, J.; Moller, D. E. The mechanisms of action of PPARs. *Annu. Rev. Med.* **2002**, *53*, 409−435.

(3) Tontonoz, P.; Spiegelman, B. M. Fat and beyond: the diverse biology of PPARγ. *Annu. Rev. Biochem.* **2008**, *77*, 289−312.

(4) Kliewer, S. A.; Sundseth, S. S.; Jones, S. A.; Brown, P. J.; Wisely, G. B.; Koble, C. S.; Devchand, P.; Wahli, W.; Willson, T. M.; Lenhard, J. M.; Lehmann, J. M. Fatty acids and eicosanoids regulate gene expression through direct interactions with peroxisome proliferator-activated receptors α and γ. *Proc. Natl. Acad. Sci. U.S.A.* **1997**, *94*, 4318−4323.

(5) Malapaka, R. R.; Khoo, S.; Zhang, J.; Choi, J. H.; Zhou, X. E.; Xu, Y.; Gong, Y.; Li, J.; Yong, E. L.; Chalmers, M. J.; Chang, L.; Resau, J. H.; Griffin, P. R.; Chen, Y. E.; Xu, H. E. Identification and mechanism of 10-carbon fatty acid as modulating ligand of peroxisome proliferator-activated receptors. *J. Biol. Chem.* **2012**, *287*, 183−195.

(6) Murphy, G. J.; Holder, J. C. PPAR-γ agonists: therapeutic role in diabetes, inflammation and cancer. *Trends Pharmacol. Sci.* **2000**, *21*, 469−474.

(7) Varga, T.; Czimmerer, Z.; Nagy, L. PPARs are a unique set of fatty acid regulated transcription factors controlling both lipid metabolism and inflammation. *Biochim. Biophys. Acta* **2011**, *1812*, 1007−1022.

(8) Cronet, P.; Petersen, J. F.; Folmer, R.; Blomberg, N.; Sjoblom, K.; Karlsson, U.; Lindstedt, E. L.; Bamberg, K. Structure of the PPARα and -γ ligand binding domain in complex with AZ 242; ligand selectivity and agonist activation in the PPAR family. *Structure* **2001**, *9*, 699−706.

(9) Ebdrup, S.; Pettersson, I.; Rasmussen, H. B.; Deussen, H. J.; Frost Jensen, A.; Mortensen, S. B.; Fleckner, J.; Pridal, L.; Nygaard, L.; Sauerberg, P. Synthesis and biological and structural characterization of the dual-acting peroxisome proliferator-activated receptor α/γ agonist ragaglitazar. *J. Med. Chem.* **2003**, *46*, 1306−1317.

(10) Nolte, R. T.; Wisely, G. B.; Westin, S.; Cobb, J. E.; Lambert, M. H.; Kurokawa, R.; Rosenfeld, M. G.; Willson, T. M.; Glass, C. K.; Milburn, M. V. Ligand binding and co-activator assembly of the peroxisome proliferator-activated receptor-γ. *Nature* **1998**, *395*, 137−143.

(11) Nagy, L.; Kao, H. Y.; Love, J. D.; Li, C.; Banayo, E.; Gooch, J. T.; Krishna, V.; Chatterjee, K.; Evans, R. M.; Schwabe, J. W. Mechanism of corepressor binding and release from nuclear hormone receptors. *Genes Dev.* **1999**, *13*, 3209−3216.

(12) Nagy, L.; Schwabe, J. W. Mechanism of the nuclear receptor molecular switch. *Trends Biochem. Sci.* **2004**, *29*, 317−324.

(13) Bruning, J. B.; Chalmers, M. J.; Prasad, S.; Busby, S. A.; Kamenecka, T. M.; He, Y.; Nettles, K. W.; Griffin, P. R. Partial agonists

activate PPARγ using a helix 12 independent mechanism. *Structure* **2007**, *15*, 1258−1271.
(14) Rangwala, S. M.; Lazar, M. A. The dawn of the SPPARMs? *Sci. STKE* **2002**, *2002*, pe9.
(15) Weidner, C.; de Groot, J. C.; Prasad, A.; Freiwald, A.; Quedenau, C.; Kliem, M.; Witzke, A.; Kodelja, V.; Han, C. T.; Giegold, S.; Baumann, M.; Klebl, B.; Siems, K.; Müller-Kuhrt, L.; Schürmann, A.; Schüler, R.; Pfeiffer, A. F.; Schroeder, F. C.; Büssow, K.; Sauer, S. Amorfrutins are potent antidiabetic dietary natural products. *Proc. Natl. Acad. Sci. U.S.A.* **2012**, *109*, 7257−7262.
(16) Lefebvre, P.; Staels, B. Naturally improving insulin resistance with amorfrutins. *Proc. Natl. Acad. Sci. U.S.A.* **2012**, *109*, 7136−7137.
(17) Mitscher, L. A.; Park, Y. H.; Al-Shamma, A.; Hudson, P. B.; Haas, T.; Amorfrutin, A. and B, bibenzyl antimicrobial agents from *Amorpha fruticosa*. *Phytochemistry* **1981**, *20*, 781−785.
(18) Kabsch, W. Automatic processing of rotation diffraction data from crystals of initially unknown symmetry and cell constants. *J. Appl. Crystallogr.* **1993**, *26*, 795−800.
(19) Vagin, A.; Teplyakov, A. MOLREP: an automated programm for molecular replacement. *J. Appl. Crystallogr.* **1997**, *30*, 1022−1025.
(20) Murshudov, G. N.; Vagin, A. A.; Dodson, E. J. Refinement of macromolecular structures by the maximum-likelihood method. *Acta Crystallogr. D* **1997**, *53*, 240−255.
(21) Adams, P. D.; Afonine, P. V.; Bunkoczi, G.; Chen, V. B.; Davis, I. W.; Echols, N.; Headd, J. J.; Hung, L. W.; Kapral, G. J.; Grosse-Kunstleve, R. W.; McCoy, A. J.; Moriarty, N. W.; Oeffner, R.; Read, R. J.; Richardson, D. C.; Richardson, J. S.; Terwilliger, T. C.; Zwart, P. H. PHENIX: a comprehensive Python-based system for macromolecular structure solution. *Acta Crystallogr. D* **2010**, *66*, 213−221.
(22) Emsley, P.; Cowtan, K. Coot: model-building tools for molecular graphics. *Acta Crystallogr. D* **2004**, *60*, 2126−2132.
(23) *The PyMOL Molecular Graphics System*, version 1.3r1; Schrodinger, LLC: New York, 2010.
(24) Wallace, A. C.; Laskowski, R. A.; Thornton, J. M. LIGPLOT: a program to generate schematic diagrams of protein-ligand interactions. *Protein Eng.* **1995**, *8*, 127−134.
(25) McLachlan, A. D. Rapid comparison of protein structures. *Acta Crystallogr. A* **1982**, *38*, 871−873.
(26) Vaguine, A. A.; Richelle, J.; Wodak, S. J. SFCHECK: a unified set of procedures for evaluating the quality of macromolecular structure-factor data and their agreement with the atomic model. *Acta Crystallogr. D* **1999**, *55*, 191−205.